J. Braz. Chem. Soc., Vol. 16, No. 1, 62-68, 2005.
Printed in Brazil - ©2005 Sociedade Brasileira de Química
0103 - 5053 $6.00+0.00

Article

Pb $^{2+}$, Cu $^{2+}$and Cd $^{2+}$ Ions Uptake by Brazilian Phosphate Rocks

Elena Mavropoulos [a], Nilce C. C. da Rocha [b], Josino C. Moreira [c], Luíz C. Bertolino [d] and Alexandre M. Rossi [,a]*

[a] *CBPF, Rua Dr Xavier Sigaud 150, Urca, 22290-180 Rio de Janeiro - RJ, Brazil.*

[b] *Instituto de Química, Universidade Federal do Rio de Janeiro, Cidade Universitária, C T, Bloco A/517, 21949-900 Rio de Janeiro - RJ, Brazil*

[c] *CESTEH/FIOCRUZ, Rua Leopoldo Bulhões 1480, 21045-900 Rio de Janeiro - RJ, Brazil.*

[d] *DGEO/FFP, Universidade Estadual do Rio de Janeiro, Rua Francisco Portela 794, 22425-000 Rio de Janeiro - RJ, Brazil*

Neste trabalho, rochas fosfatadas brasileiras (PRs) foram usadas na imobilização de Pb^{2+}, Cu^{2+} e Cd^{2+} de soluções aquosas. Concluímos que estes metais são principalmente imobilizados por fluorapatita, mas outros minerais tais com carbonatos de cálcio contribuem para esta imobilização. No caso do chumbo, dois mecanismos são propostos: a dissolução da $Ca_{10}(PO_4)_6F_2$ seguida pela precipitação de $(Ca,Pb)_{10}(PO_4,CO_3)_6(OH,F,Cl)_{2.56}.1.5H_2O$ e a dissolução de $CaCO_3$ com formação de $PbCO_3$. Este segundo mecanismo aumenta a eficiência do processo de remoção, mas contribui para tornar o chumbo mais biodisponível porque o carbonato de chumbo é mais solúvel que a fluorpiromorfita. Este fato pode limitar a utilização das rochas fosfatadas na regeneração de solos contaminados. A imobilização de Cu^{2+} e do Cd^{2+} pelas PRs é controlada por mecanismos de adsorção mas mecanismos de dissolução/precipitação também contribuem. No caso do Cu^{2+} a dissolução da fluorapatita é seguida pela precipitação da libetenita, $Cu_2(PO_4)(OH)$.

In this work Brazilian phosphate rocks, PRs, were used to reduce Pb^{2+}, Cu^{2+} and Cd^{2+} concentrations from aqueous solutions. We concluded that these metals were mainly immobilized by fluorapatite but other minerals such as calcium carbonate also contribute to their immobilization. In the case of lead two mechanisms are proposed: the $Ca_{10}(PO_4)_6F_2$ dissolution followed by the precipitation of $(Ca,Pb)_{10}(PO_4,CO_3)_6(OH,F,Cl)_{2.56}.1.5H_2O$ and $CaCO_3$ dissolution with the formation of a $PbCO_3$. The occurrence of this second mechanism improves the uptake efficiency but contribute to the increases of lead bioavailability because lead carbonate is more soluble than fluorpyromorphite. This fact could limit the use of PRs for remediation of contaminated soils and wastes. The Cu^{2+} and Cd^{2+} removal by PRs is controlled by adsorption mechanisms but dissolution /precipitation mechanisms also occur. In the case of Cu^{2+}, fluorapatite dissolution followed by $Cu_2(PO_4)(OH)$ precipitation.

Keywords: lead, cadmium and cooper immobilization, phosphate rock, hydroxyapatite

Introduction

The increasing rate of the environment pollution has stimulated worldwide research concerning new materials capable to remove heavy metals from contaminated soils and wastes. Several studies have shown that synthetic hydroxyapatite, HA, have potential for remediation applications because it can immobilize a great number of heavy metals [1-3] from aqueous media by forming new low soluble phosphates phases. However, the use of synthetic HA in technological applications is only feasible when a small quantity of material is used because HA preparation is rather expensive. For this reason, low cost materials like phosphate rocks, PRs, have been proposed and tested for heavy metal removal from contaminated waste and soils.[4,5] When the remediation properties of PR are investigated some questions are normally discussed. Could PRs be efficient enough to immobilize heavy metals as synthetic HA is? Is metal immobilization dependent on the PR mineralogical and chemical composition? Do apatite minerals always control the mechanism of metal immobilization?

Several authors made relevant contributions to this

* e-mail: rossi@cbpf.br

discussion showing that PR was very effective in retaining Pb and less effective in the removal Cd and Zn from aqueous solutions.[6] The Pb^{2+} immobilization was mainly controlled by apatite dissolution and the precipitation of a carbonated fluoropyromorphite.[7,8] Recently, in situ studies have been conducted with success.[8–12] However, the use of PRs in remediation of soils and wastes does not only depend on the effectiveness of the removal process but mainly on the stability of the new metal phases formed. A high bioavailability of this new metal phase could limit the use of PRs *in situ* applications.

In this work, we showed that depending on PRs composition, other minerals might compete with apatite for metal removal. For this, we investigate the effectiveness of PRs samples from the southeast (São Paulo and Minas Gerais States) central west and northeast (Goiás and Bahia States) of Brazil in attenuating Pb^{2+}, Cu^{2+} and Cd^{2+} from aqueous solution. A comparative study concerning the immobilization process of PR and synthetic apatite was also performed. The uptake experiments were carried out with different grain size fractions of PR in order to identify the minerals that participate in the Pb^{2+}, Cu^{2+} and Cd^{2+} removal. Discussion about the uptake mechanisms of Pb^{2+}, Cu^{2+} and Cd^{2+} by Brazilian PRs and their potential for remediation applications was carried out.

Experimental

Sample preparation

Five PRs from different Brazilian regions were studied. PRA sample was collected in a Cretaceous igneous-alkaline deposit situated in Tapira region, Minas Gerais State. The PRB and PRE samples belong to an igneous-alkaline complex of Cretaceous Superior from Goias State.[13] The PRD and PRC samples came from Bahia and Minas Gerais States deposits, respectively. They are from Medium and Superior Proterozoic and have sedimentary origins. The PRs samples were obtained in form of a heterogeneous powder of coarse particles. Samples were homogenized in agate grail and separated in six grain fractions: PR_1 (<0.074 mm), PR_2 (0.074-0.125 mm), PR_3 (0.125-0.177 mm) PR_4 (0.177-0.210 mm), PR_5 (0.210-0.250 mm) and PR_6 (0.250-2.00 mm). Their BET surface areas were 16.1, 13.7, 11.4, 9.2, 4.6 and 8.7 $m^2\ g^{-1}$, respectively.

Synthetic hydroxyapatite (HA) samples were synthesized by drop wise addition of an $(NH_4)_2HPO_4$ aqueous solution to a $Ca(NO_3)_2$ solution (both reagents PA Merck) at 80 °C and pH 11. It was a pure HA with a Ca/P molar ratio of 1.65 ± 0.03 and surface area BET of 45 ± 4 $m^2\ g^{-1}$.

Sample characterization

The PRs and HA samples were analyzed by a SEIFERT-FPM GmbH X-ray diffractometer (XRD), operating with CuKα radiation (1.5418 Å) at 40 kV and 40 mA with a graphite monochromator in the primary bunch. The XRD patterns were obtained in an interval from 10 to 100° with 2θ step of 0.02°. The apatite and calcite crystallite mean sizes were determined using Scherer equation. Elementary chemical analysis of Ca and P content and other elements were determined by ICP-OES using equipment OPTIMA 3000 PERKIN-ELMER. Sample thin section were prepared and analyzed with polarizing microscope Carl Zeiss Axioplan.

Dissolution experiments

Dissolution experiments in Milli-Q water were accomplished in triplicate, using 0.2 g of synthetic HA, PRA and PRA_1 samples. They were mechanically shaken in 40 mL tubes during 10 days. After 4, 24, 48, 72, 168 and 240 hours solution aliquots were collected, filtered using a 0.22 μm Durapore membrane Millipore and diluted in HNO_3 0.25%. The Ca and P content were then determined by ICP-OES. The pH was monitored during HA, PR and PR finest fractions (PR_1) dissolution in Milli-Q water using a calibrated pH meter Analyser-300 M.

Uptake, desorption and pH experiments

The uptake experiments using HA, PRA and its fractions (PRA_i) were performed in triplicate using 0.2 g of each sample. Aqueous solutions (40 mL) containing Pb^{2+} (2.43×10^{-3} mol L^{-1}), Cu^{2+} (5.16×10^{-3} mol L^{-1}) and Cd^{2+} (2.67×10^{-3} mol L^{-1}), obtained from $Pb(NO_3)_2$, $Cu(NO_3)_2.3H_2O$ and $Cd(NO_3)_2.4H_2O$, were mechanically shaken up to 10 days. The sample suspensions were centrifuged and the supernatants were filtered using a 0.22 μm membrane Millipore, diluted with HNO_3 0.25% and then analyzed by ICP. The solid residues were dried at 80 ºC and analyzed by XRD. The same procedure was used in a second series of experiments in order to evaluate the uptake capacity of Pb^{2+}, Cu^{2+} and Cd^{2+} by HA and PRA. These 240 hours experiments used Pb^{2+}, Cu^{2+} and Cd^{2+} initial concentrations of 0.94-1.50×10^{-3} mol L^{-1}, 0.71-4.33×10^{-3} mol L^{-1} and 0.91-2.36×10^{-3} mol L^{-1}, respectively.

A third series of experiments was performed to estimate the uptake effectiveness of each one of the PRs (PRA, PRB, PRC, PRD and PRE) and their finest fractions (PRA_1, PRB_1, PRC_1, PRD_1 and PRE_1). Solutions containing Pb^{2+} 1.46×10^{-3} mol L^{-1}, Cu^{2+} 0.85×10^{-3} mol L^{-1} and Cd^{2+} 0.78×10^{-3} mol L^{-1}

were used in these 3 days experiments. The sample suspensions and the solid residues were treated and analyzed by ICP and XRD as described before.

The metal selectivity along the uptake process was investigated by the following procedure: 0.2 g of HA, PRA and PRA_1 were added to 40 mL of an aqueous solutions containing nearly 1×10^{-3} mol L^{-1} of Pb^{2+}, Cu^{2+} and Cd^{2+}. Supernatants aliquots were withdrawn from solution after 72 hours of reaction and analyzed by ICP. The availability of Pb^{2+}, Cu^{2+} and Cd^{2+} by PR was also investigated: after uptake, the sample was washed in Milli-Q water and centrifuged. The solid was added to 40 mL of Milli-Q water and maintained under agitation during 7 days. Afterwards, the solutions were separated from solid and analyzed by ICP. The pH was monitored during the uptake experiments as described before.

Results and Discussion

Mineralogical and structural characterization

Thin section analyses showed that PRs were composed by apatite, mica, goethite, magnetite, calcite and quartz. The most abundant elements of PRs were Ca, P, Fe and Al but other metals like Cr, Ni, Zn, Pb, Cu and Cd were also presented in small amounts (Table 1). Ca and P contents were highly variable among the studied samples. Morphological characterization revealed that PR had a threemodal particle size distribution with maximum centered at 130, 36 and 4 μm while synthetic HA had a bimodal particle size distribution with maximum centered at 4 and 23 μm. Particles with dimensions around 4 μm were mainly presented in synthetic HA but contributed weakly in the PRA and PRA_1 fractions.

Differently from others PRs already studied [6-8] the Brazilian PRs were mainly composed by fluorapatite, $Ca_{10}(PO_4)_6F$. In one sample a small substitution of F^- by OH^- and PO_4^{3-} by CO_3^{2-} was observed by XRD. No other phosphate was detected by XRD. Quartz peaks were detected in all XRD patterns with relative intensities varying in the following order: PRE>PRA>PRD>PRC>PRB. Peaks of calcite were identified in the PRB and PRD samples. Among PR_1 fractions, calcite peaks were mainly concentrated in samples PRA_1 and PRD_1 as ultra fine particles with mean crystal size of 64 nm.

The fluorapatite relative content of PRs was estimated by XRD by comparing peaks intensity at $2\theta = 31.94$ (100%), $2\theta = 32.26$ (55%) and $2\theta = 33.11$ (60%). In samples PRB and PRA, fluorapatite was mainly concentrated in the large and small particle size fractions, respectively. It

Table 1. Material characterization

Sample	BET Area (m^2g^{-1})	Grainy (mm)	Most Abundant Elements g kg^{-1}									
			Ca	P	Cu	Cd	Cr	Ni	Pb	Zn	Al	Fe
HA	45.0 ±0.1	<0.210	396	187	nd	nd	nd	nd	nd	nd	nd	nd
PRA	9.5 ±0.04	<0.210	117 ±0.29	32.7 ±0.19	0.02 $\pm9\times10^{-4}$	bd	bd	0.05 $\pm3\times10^{-4}$	0.03 $\pm2\times10^{-3}$	0.12 $\pm2\times10^{-4}$	14.2 $\pm2\times10^{-4}$	121 ±0.29
PRA_1	16.1 ±0.07	<0.074	133 ±0.31	37.6 ±0.16	0.04 $\pm5\times10^{-4}$	0.01 $\pm1\times10^{-4}$	bd	0.06 $\pm2\times10^{-4}$	0.05 $\pm5\times10^{-3}$	0.14 $\pm2\times10^{-4}$	17.3 ±0.04	114 ±0.2
PRB	12.5 ±0.03	<0.210	116 ±0.06	45.4 ±0.06	0.15 $\pm9\times10^{-4}$	0.02 $\pm6\times10^{-5}$	0.19 $\pm2\times10^{-4}$	0.22 $\pm4\times10^{-3}$	0.10 $\pm2\times10^{-3}$	0.28 $\pm4\times10^{-4}$	10.0 ±0.05	193 ±0.1
PRB_1	20.0 ±0.06	<0.074	94.7 ±0.26	40.2 ±0.20	0.32 $\pm6\times10^{-4}$	0.01 $\pm2\times10^{-5}$	0.19 $\pm1\times10^{-4}$	0.38 $\pm2\times10^{-3}$	0.17 $\pm3\times10^{-3}$	0.40 $\pm1\times10^{-3}$	19.3 ±0.05	209 ±0.50
PRC	4.0 ±0.02	<0.210	335 ±0.42	126 ±0.45	bd	bd	bd	0.03 $\pm5\times10^{-4}$	bd	0.12 $\pm1\times10^{-4}$	12.5 ±0.05	8.20 ±0.05
PRC_1	6.7 ±0.01	<0.074	300 ±0.24	110 ±0.21	0.01 $\pm2\times10^{-4}$	bd	0.01 $\pm2\times10^{-4}$	0.06 $\pm5\times10^{-4}$	bd	0.16 $\pm2\times10^{-4}$	19.0 ±0.16	15.2 ±0.07
PRD	6.0 ±0.01	<0.210	331 ±2.6	122 ±0.91	bd	bd	0.02 $\pm1\times10^{-4}$	bd	bd	0.02 $\pm1\times10^{-4}$	9.95 ±0.10	5.74 ±0.03
PRD_1	20.0 ±0.05	<0.074	286 ±0.97	96.8 ±0.50	0.02 $\pm3\times10^{-4}$	bd	0.04 $\pm2\times10^{-4}$	0.02 $\pm5\times10^{-4}$	0.02 $\pm1\times10^{-3}$	0.04 $\pm2\times10^{-5}$	28.5 ±0.14	17.3 ±0.06
PRE	9.0 ±0.04	<0.210	125 ±0.11	44.0 ±0.11	0.40 $\pm3\times10^{-3}$	0.01 $\pm5\times10^{-5}$	0.34 $\pm7\times10^{-4}$	0.31 $\pm2\times10^{-3}$	0.1 $\pm2\times10^{-3}$	0.30 $\pm1\times10^{-3}$	10.4 ±0.06	173 ±0.11
PRE_1	14.0 ±0.05	<0.074	144 ±0.40	54.8 ±0.18	0.51 $\pm4\times10^{-3}$	0.01 $\pm5\times10^{-5}$	0.28 $\pm4\times10^{-4}$	0.34 $\pm1\times10^{-3}$	0.20 $\pm2\times10^{-3}$	0.32 $\pm7\times10^{-4}$	8.45 ±0.02	165 ±0.38

nd=not determined; bd=below detection.

was homogeneously distributed between raw and fine fractions in sample PRC, PRD and PRE. The XRD analysis revealed that fluorapatite crystals had larger crystallite dimensions (50 nm along 002 direction) and lower specific surface areas than synthetic HA. This improvement on PR crystallinity and crystallite dimension was probably due to thermal treatments submitted by PR during their geological genesis.

Dissolution of PR and pH behavior during metal uptake

Dissolution rate and pH are important parameters to understand the mechanism and effectiveness of heavy metals removal by PRs in water solutions.[9,11,14,15] In the present work, dissolution experiments showed that dissolution rate was strongly variable among PRs samples but was not directly related to sample Ca or P contents. The variations were more pronounced in respect to the amount of Ca released to the solution than to P, due to the existence of more soluble Ca-compounds such as $CaCO_3$ in some of the PRs like samples PRA and PRD. Dissolution experiments in Milli-Q water using samples PRA and PRA_1 showed that the equilibrium of Ca and P was no longer achieved even for dissolution times up to 240 hours (data not shown). The dissolution Ca/P ratio for PRA (Ca/P=11.50) and PRA_1 (Ca/P=10.30) was higher than that of HA (Ca/P=0.39), which should be due to the contribution of other Ca-compounds existing in PR beside apatite. This explains why PRA_1 released twice more Ca^{2+} than synthetic HA but was less efficient in releasing P. Dissolution data also revealed that the release of Ca and P was mostly originated from sample fine fractions, which were rich in apatite and carbonate minerals.

The pH increased rapidly when PRs were dissolved in Milli-Q water due to the presence of basic minerals (Table 2). It varied from 6.2 to 9.2 and reached its highest values for PRA_1 and PRD_1 samples, which had the highest calcite contents. In the beginning of the Pb^{2+}, Cu^{2+} or Cd^{2+} immobilization by HA, Table 3, the pH decreased indicating that metal complexation at HA surface [2] was so efficient as apatite dissolution.[16,17] The same behavior was only seen in the beginning of Pb^{2+} immobilization by PRA. For Cu^{2+} and Cd^{2+} immobilization by PRA and PRA_1 the pH increased continuously indicating that the decrease of pH due to metal complexation was neutralized by carbonate minerals dissolution, as was observed in dissolution experiments (Table 2).

Uptake and desorption experiments

Sorption experiments using PRA sample showed (Figure 1 and Table 4), that the removal of Pb^{2+}, Cu^{2+} and Cd^{2+} was dependent on metal initial concentration and the uptake time. The Pb^{2+} uptake was 30% lower than synthetic HA in the first 4 hours of the kinetic process but achieved 90% at the end of 72 hours (Table 4). It increased with the decrease of PR grain size (Figure 2), and the highest immobilization occurs for R_1 fraction, which was rich in fluorapatite.

The Pb^{2+} immobilization by PRs, Figure 3, was strongly variable and decreased in the following order: PRA>PRB>PRE>PRD>PRC. The uptake effectiveness of raw samples and their fine fractions varied from 5 mg g^{-1} (PRC) to 36 mg g^{-1} (PRA) and from 6 mg g^{-1} (PRC_1) to 57 mg g^{-1} (PRA_1), respectively. These variations could not be attributed to sample Ca or P contents or to sample surface area because samples PRB_1 and PRA_1 had similar BET areas but PRA_1 immobilized 2.5 times more Pb than PRB_1. In addition, PRA sample had smaller Ca and P contents

Table 2. Variation of the solution pH during dissolution of PR finest fractions in Milli-Q water. The estimated error is ± 0.05

time (minute)	PR Finest Fractions (Pr_1)					
	PRA_1	PRB_1	PRC_1	PRD_1	PRE_1	HA
0	6.2	6.2	6.2	6.2	6.2	6.2
1	8.2	6.44	6.3	7.73	6.78	7.36
5	9.19	7.03	6.7	9.12	7.42	7.48
30	9.08	6.86	7.15	8.83	7.15	7.5
60	8.96	7.06	7.09	8.85	7.05	7.5
1440	8.28	7.2	7.47	8.17	7.41	7.54
2880	8.31	7.08	7.44	8.15	7.48	7.52

Table 3. Variation of the solution pH during sorption experiments of Pb^{2+}, Cu^{2+} and Cd^{2+} by HA, PRA and PRA_1. The estimated error is ± 0.05

time (minute)	HA			PRA			PRA_1		
	Pb	*Cu*	*Cd*	*Pb*	*Cu*	*Cd*	*Pb*	*Cu*	*Cd*
0	5.22	5.29	5.69	5.22	5.28	5.73	5.11	5.29	5.72
1	4.46	4.77	5.14	5.15	5.32	6.25	5.13	5.29	6.13
3	5.67	4.86	5.27	5.29	5.35	6.32	5.23	5.34	6.26
5	5.79	4.96	5.33	5.37	5.44	6.35	5.28	5.37	6.31
15	5.9	5.27	5.38	5.5	5.52	6.34	5.43	5.44	6.3
30	5.93	5.36	5.46	5.52	5.69	6.34	5.49	5.49	6.29
60	5.95	5.4	5.6	5.63	5.73	6.38	5.53	5.61	6.29

Table 4. Pb^{2+}, Cu^{2+} and Cd^{2+} uptake and desorption by HA and PRA samples

Metal	Initial Conc.	%Uptake				%Desorption	
	mol L^{-1} $\times10^{-3}$	HA		PRA		HA	PRA
		4h	72h	4h	72h		
Pb^{2+}	0.94	100(±0.02)	100(±0.02)	72(±1.32)	90(±0.34)	bd	0.2(±0.01)
	1.26	100(±0.02)	100(±0.02)	59(±0.29)	77(±0.63)	bd	0.2(±0.01)
	1.50	100(±0.02)	100(±0.02)	57(±0.52)	76(±0.22)	bd	1.2(±0.08)
Cu^{2+}	0.71	99(±0.09)	100(±0.02)	72(±0.84)	99(±0.14)	0.2(±0.01)	0.9(±0.02)
	4.33	37(±2.45)	96(±0.20)	12(±1.73)	32(±2.00)	bd	0.4(±0.06)
Cd^{2+}	0.91	97(±0.15)	98(±0.03)	43(±0.59)	45(±0.55)	2.1(±0.16)	7.1(±0.42)
	2.36	56(±0.58)	63(±1.06)	14(±2.61)	16(±2.27)	0.5(±0.10)	4.7(±0.15)

bd=below detection

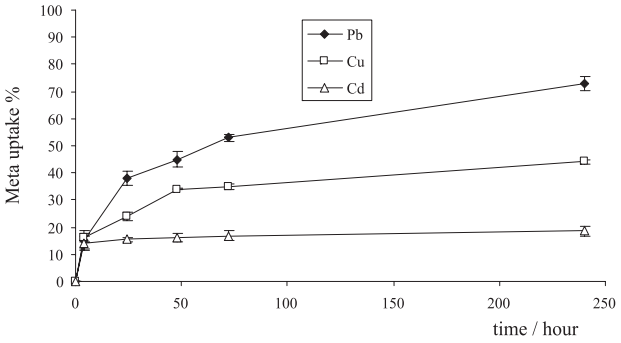

Figure 1. Pb^{2+}, Cu^{2+} and Cd^{2+} immobilization by sample PRA, 240 hours uptake experiments using metal initial concentration of 1.26×10^{-3} mol L^{-1}, 4.33×10^{-3} mol L^{-1} and 2.36×10^{-3} mol L^{-1}, respectively.

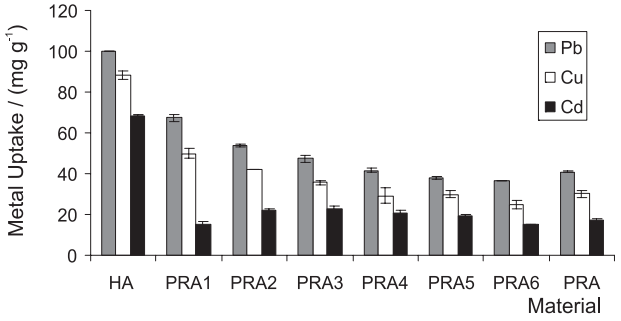

Figure 2. Pb^{2+}, Cu^{2+} and Cd^{2+} uptake by synthetic HA and PRA grain fractions $PRA_{1\text{-}6}$. Metal initial concentration of 2.43×10^{-3} mol L^{-1}, 5.16×10^{-3} mol L^{-1} and 2.67×10^{-3} mol L^{-1}, respectively.

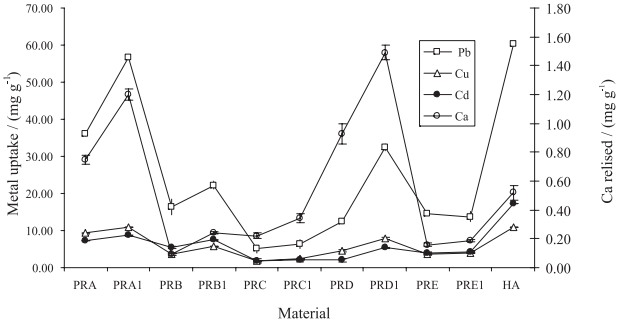

Figure 3. Pb^{2+}, Cu^{2+} and Cd^{2+} immobilization (48 hours) by phosphate rocks and their finest fractions (PR_1) as function of calcium released to Milli-Q water: (○) Ca^{2+}, (□) Pb^{2+}, (△) $Cu^{2+}$and (●) Cd^{2+}. Initial concentration of Pb^{2+}, Cu^{2+} and Cd^{2+} of 1.46×10^{-3} mol L^{-1}, Cu^{2+} 0.85×10^{-3} mol L^{-1} and Cd^{2+} 0.78×10^{-3} mol L^{-1}, respectively.

than the PRC sample but immobilized about 7 times more Pb. Figure 3 also revealed that the removal efficiency was not influenced by sample geological origin: samples PRD and PRE showed similar Pb^{2+} uptake effectiveness but had sedimentary and igneous origins, respectively. The data of Figure 3 confirmed that Pb^{2+} is mainly immobilized by PRs fine fractions and also suggested a correlation between the dissolution of Ca-compounds and the Pb^{2+} removal from aqueous solution. However, the Pb^{2+} removal was not directly related to fluorapatite content of PR: PRC_1 showed a similar fluorapatite content as PRA_1 but immobilized 9 times less Pb^{2+}. This supports the proposal that other soluble Ca-compounds besides fluorapatite should also play a relevant role in Pb immobilization by PRs.

Comparing results of Table 2 and Figure 3 we verified that the high effectiveness of PR in removing Pb^{2+} was not linked to the low pH levels of the solution. Two cases exemplified this hypothesis: the PRA_1 and PRD_1 samples showed the highest Pb^{2+} uptake whereas pH was kept in high levels during the uptake process (Table 3). These results, which are in opposition to previous works,[1,3,14] can be understood by the role of other minerals of PRs during the uptake process.

The comparison between the XRD patterns of PR samples, before and after Pb^{2+} uptake, was essential to clarify the previous results as well as to detail the mechanisms of Pb^{2+} immobilization. One example was the XRD pattern of sample PRA_1 after the Pb^{2+} uptake. It showed an additional peak at $2\theta = 30.91$ and a modification in the relative intensity of the fluorapatite peaks at $2\theta = 31.94$, $2\theta = 32.26$ and $2\theta = 33.11$ in relation to non-treated sample. This changes was attributed to the formation of a solid solution of Ca and Pb such as $(Ca,Pb)_{10}(PO_4,CO_3)_6(OH,F,Cl)_{2.56}.1.5H_2O$.[16] In addition to this fluorapatite solid solution, the XRD patterns of the PRA and PRD samples also showed two intense peaks at

$2\theta = 24.83$ and $2\theta = 25.53$, which were assigned to a cerussite phase, $PbCO_3$.

These above results indicated that Pb^{2+} uptake by PRs involves not only one but two mechanisms: the dissolution of fluorapatite and calcite followed by precipitation of a Ca and Pb apatite solid solution and cerussite. The occurrence of these simultaneous reactions should have relevant consequences to lead immobilization by PRs. The first consequence was that calcium carbonate rich PRs samples should leads to high Pb^{2+} uptake levels. This hypothesis is confirmed by results of Figure 3, which showed that carbonate rich samples PRA_1 and PRD_1 immobilized much more lead (32-57 mg g^{-1}) than low carbonate content ones (5-17 mg g^{-1}). The second consequence was that lead bioavailability should increase in these samples because lead carbonate minerals are more soluble than lead apatite. This may constitute an important limitation for PRs when used in soil and wastes remediation. Hence, additional studies must to be done to estimate the release of lead from lead carbonate in complex systems like soils during long-term experiments.

For low metal concentration (<1x10^{-3} mol L^{-1}) and reaction time of 4 hours, Cu^{2+} presented uptake effectiveness as higher as Pb (Table 4). The Cu^{2+} uptake effectiveness was ordered as HA>PRA>PRB>PRE>PRD>PRC (Figure 3), and increased with the decrease of PR grain size, achieving a maximum for PRA_1 fraction (Figure 2 and 3). This reinforced the hypothesis that apatite minerals primarily immobilized Cu^{2+}. XRD analysis performed in synthetic HA samples after several days of Cu^{2+} uptake showed a reduction of HA peaks intensity and the appearance of peaks attributed to libethenite, $Cu_2(PO_4)(OH)$ (Figure 4). This indicated that dissolution/precipitation mechanisms are also involved in Cu^{2+} immobilization besides metal adsorption in apatite surface.

The Cd^{2+} uptake was fast but achieved saturation in the first 4 hours of reaction (Figure 1). For initial concentration of nearly 1x10^{-3} mol L^{-1}, the Cd^{2+} uptake by PRA was about 50% less effective than Pb^{2+} and Cu^{2+} (Table 4). The fine fraction was not the most efficient for the Cd^{2+} immobilization (Figure 2), contrasting with its behavior during the Pb^{2+} and Cu^{2+} uptake. This suggested

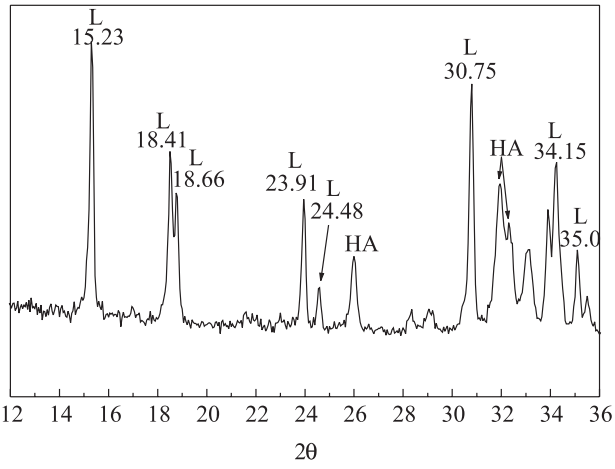

Figure 4. XRD pattern of synthetic HA after 10 days uptake experiments showing hydroxyapatite (HA) and libethenite (L) peaks. Solution containing 0.2g HA and Cu^{2+} initial concentration of 9.84×10^{-3} mol L^{-1}.

that apatite minerals did not control Cd^{2+} uptake. The XRD analyses performed in PR samples after the Cd^{2+} uptake did not show peaks of new Cd phases such as Cd-apatite or Cd-carbonate. On the other hand, the Cd^{2+} uptake was not linked to the dissolution of Ca^{2+} complexes, as shown in Figure 3. Both results supported the proposal that Cd^{2+} uptake was not dependent on dissolution/precipitation mechanisms as in the case of $Pb^{2+}$and Cu^{2+}. As a consequence, adsorption mechanisms like surface complexation or ionic exchange [2,17-20] should control Cd^{2+} immobilization. The behavior of Cd^{2+} in desorption experiments reinforced this hypothesis because PRs were more efficient in release Cd^{2+} to solution (7%) than Pb^{2+} and Cu^{2+} (2%).

Selectivity uptake experiments were carried out with Pb^{2+}, $Cu^{2+}$and Cd^{2+} simultaneously present in a solution containing synthetic HA. As shown in Table 5, the Pb^{2+} uptake by HA was not altered by the presence of the other metals in the solution. In contrast, Cu^{2+} and Cd^{2+} removal capacity decreased by 22% and 59% respectively. When PRA fraction was used in a similar experiment the Pb^{2+}, Cu^{2+} and Cd^{2+} uptake presented a decrease of about 25%, 60% and 75% respectively in comparison to isolate metal uptake (Table 5). These results suggest that PR uptake

Table 5. Results of 72 hours uptake experiments with Pb^{2+}, Cu^{2+} and Cd^{2+} coexisting in aqueous solution. Metal initial concentration of 0.97×10^{-3} mol L^{-1} (Pb^{2+}), 1.01×10^{-3} mol L^{-1} (Cu^{2+}) and 0.94×10^{-3} mol L^{-1} (Cd^{2+}). Metal desorption after 7 days

Material	Uptake%			Desorption%		
	Pb^{2+}	Cu^{2+}	Cd^{2+}	Pb^{2+}	Cu^{2+}	Cd^{2+}
HA	100(±0.02)	78(±2.29)	40(±0.39)	Bd	0.6(±0.01)	4.0(±0.08)
PRA	68(±0.76)	40(±1.47)	11(±0.59)	0.9(±0.08)	1.2(±0.08)	19.5(±1.58)
PRA_1	91(±0.85)	63(±0.65)	15(±1.07)	0.9(±0.08)	0.1(±0.01)	5.1(±0.09)

effectiveness could be strongly affected when Pb^{2+}, Cu^{2+} and Cd^{2+} are in contact with a more complex media.

Conclusions

From the above results we can conclude that Brazilian PR had high efficiency in immobilizing Pb^{2+}, Cu^{2+} and Cd^{2+} from aqueous media. The existence of an ultra fine fraction of calcium carbonate in some of PRs contributed to improve their efficiency in removing Pb^{2+} because the uptake was not only exclusively controlled by the Ca-apatite dissolution and Pb-apatite precipitation but also by the calcium carbonate dissolution and the precipitation of lead carbonate. Cu^{2+} was also immobilized by mechanisms such as dissolution/precipitation with the formation of libethenite. Other minerals contribute to Cd^{2+} immobilization besides fluorapatite. These results indicated that soluble minerals containing in PR composition compete with apatite in metal immobilization processes. This could be an important limitation for using PRs *in situ* remediation.

Acknowledgements

The authors wish to thank CNPq, Centro de Pesquisas e Desenvolvimento Leopoldo A. M. de Mello da Petrobras and EMBRAPA/SOLOS for financial add and sample characterization.

References

1. Ma, Q. Y.; Traina, S.J; Logan, T. J.; Ryan, J. A.; *Environ. Sci. Technol.* **1993**, *27*, 1803.
2. Xu, Y.; Schwartz, F. W.; Traina, S. J.; *Environ. Sci. Technol*. **1994**, *28*, 1472.
3. Xu, Y.; Schwartz, F. W.; *J. Contam. Hydrol.* **1994**, *15*, 187.
4. Laperche, V.; Logan, T. J.; Gaddam, P.; Traina, S. J.; *Environ. Sci. Technol*. **1997**, *31*, 2745.
5. Reichert, J.; Binner, J. G. P.; *J. Mater. Sci.* **1996**, *31*, 1231.
6. Chen, X.; Wright, J. V.; Conca, J. L.; Peurrung, L. M.; *Water Air Soil Pollut*. **1997**, *98*, 57.
7. Ma, L. Q.; Rao, G. N.; *Water Air Soil Pollut*. **1999**, *110*, 01.
8. Ma, Q. Y.; Logan, T. J.; Traina, S. J.; *Environ. Sci. Technol*. **1995**, *29*, 1118.
9. Cao, R. X.; Ma, L. Q.; Chen, M.; Singh, S. P.; Harris, W. G.; *Environ. Pollution* **2003**, *122*, 19.
10. Chen, M.; Ma, L. Q.; Singh P. S.; Cao, R. X.; Melamed, R.; *Adv. Environ. Res.* **2003**, *8*, 93.
11. Cao, X.; Ma, L. Q.; Chen, M.; Singh, S. P.; Harris, W. G.; *Environ. Sci Technol*. **2002**, *36*, 5296.
12. Melaned, R.; Cao, X.; Chen, M.; Ma, Q. L.; *Sci. Total Environ*. **2003**, *305,* 117.
13. Melo, M. T. V. *Depósitos de Fosfato, Titânio e Nióbio de Tapira, Minas Gerais; Departamento Nacional da Produção Mineral. Principais Depósitos Minerais do Brasil*; Rochas e Minerais Industriais, vol IV, Co-edição DNPM/CPRM: Brasília, 1997, p. 41-56.
14. Chen, X., J. V. Wright, J. L. Conca; Peurrung, L. M.; *Environ. Sci Technol*. **1997**, *31*, 624.
15. Zhang, P; Ryan, J. A.; Yang, J.; *Environ. Sci. Technol*. **1998**, *32*, 2763.
16. Mavropoulos, E.; Rossi, A. M., Costa, A. M.; Perez, C. A. C.; Moreira, J. C.; Saldanha, M.; *Environ. Sci. Technol.* **2002**, *36*, 1625.
17. Rocha, N. C. C.; Campos, R. C. C.; Rossi, A. M., Moreira, E. L.; Barbosa, A. F.; Moure, G. T.; *Environ. Sci. Technol.* **2002**, *36*, 1625.
18. Xu, Y.; *PhD. Thesis*, The Ohio State University, USA, 1994.
19. Jeanjean, J.; Fedoroff, M.; Faverjon, F.; Vincent, U.; *J. Mater. Sci*. **1996**, *31*, 6156.
20. Toulhoat, N.; Potocek, V.; Neskovic, C.; *Radiochim. Acta* **1996**, *74*, 257.

Received: October 10, 2003
Published on the web: December 16, 2004